Int. J. Electrochem. Sci., 7 **(2012)** 8276 - 8287

International Journal of
ELECTROCHEMICAL
SCIENCE
www.electrochemsci.org

Synthesis, Characterization, Morphology and Photovoltaic Properties of Aniline-Tiophene Based Polymers

P.P. Zamora[1,*], *M.B. Camarada*[2], *I.A. Jessop*[1], *F. R. Díaz*[1], *M.A. del Valle*[21], *L. Cattin*[3], *G. Louarn*[3] *and J.C Bernede*[4]

[1] Pontificia Universidad Católica de Chile, Facultad de Química, Departamento de Química Orgánica, Laboratorio de Polímeros, Av. Vicuña Mackenna 4860, Santiago de Chile
[2] Pontificia Universidad Católica de Chile, Facultad de Química, Departamento de Química Inorgánica, Laboratorio de Electroquímica de Polímeros, Av. Vicuña Mackenna 4860, Santiago de Chile
[3] Université de Nantes, LUNAM Université, Institut des Matériaux de Nantes, CNRS, 2 rue de la Houssinière, BP 32229, 44322 Nantes cedex 3, France
[4] Université de Nantes, LUNAM Université, MOLTECH-Anjou, CNRS, UMR 6200, 2 rue de la Houssinière, BP 92208, Nantes, F-44000 France
[*]E-mail: ppzamora@uc.cl

Received: 13 July 2012 / *Accepted:* 16 August 2012 / *Published:* 1 September 2012

Monomers composed of thiophene and aniline rings, 4-(2-thiophen)aniline and 4-(3-thiophen)aniline, were successfully synthetized through the *Suzuki-Miyaura* cross coupling reaction and then polymerized. The polymers poly 4-(2-tiophen)aniline and poly 4-(3-tiophen)aniline (P4,2TA and P4,3TA) were characterized via spectroscopycal NMR, optical and electrochemical methodologies. Subsequently the morphology of deposits were characterized using atomic force microscopy (AFM) and X-ray diffraction (XRD). The photovoltaic devices were constructed under the same conditions, observing differences in the photovoltaic yield of each polymer. P4,2TA exhibited higher photovoltaic yield in comparison with P4,3TA, indicating that the molecular geometry affects the crystallinity and surface morphology of the polymeric deposits, and the photovoltaic properties

Keywords: conducting polymers, morphology, XRD, electrochemistry, photovoltaic yield

1. INTRODUCTION

Conducting polymers are flexible and low-cost materials for use in electronic applications. Electronically conducting heteroatomic based polymers, such as poly(aniline) and poly(thiophene), have become increasingly studied in both academic and industrial fields because of their stability, high

conductivity and tunable optical properties. Poly(aniline) has been applied in a number of commercial applications such as sensors, rechargeable batteries, electrochromic displays, selective membranes, charge dissipative coatings and corrosion resistant coatings[1-4], however, it has no photovoltaic properties.

Poly(thiophene) have attracted particular attention, due to its high processability, outstanding environmental stability and low band gap value. Its applications are wide-ranging and include surface light emitting diodes (SLED's)[5], light emitting diodes (LED's)[6-12], photovoltaic cells[13-17] and transistors[18-24].

It is well known that aniline is an electron donor, while thiophene is an electron acceptor. Then, a π-conjugated thiophene/aniline-based polymer, as poly 4-(2-thiophen)-aniline (P4,2TA) and poly 4-(3-thiophen)-aniline (P4,3TA), having both properties (electron donor and acceptor) at the same molecule, will exhibit a reduced *band gap* (*Eg*)[25-27]. For this reason, thiophene/aniline-based polymers are materials with photoelectrical properties that could be used in solar cells as sandwiched active layer between two electrodes with different work functions. To accelerate the efforts in technology development and succeed in the designing of new and improved materials, it is significant to find the relationship between photoelectrical properties, electronic structure and morphology, which is very important to establish a good contact between the electron donor and the electron acceptor[28].

The highest occupied molecular orbital (HOMO) energy, the lowest unoccupied molecular orbital (LUMO) energy and the energy gap between both levels, are the appropriate parameters to understand and control the optical, electrical and chemical properties of polymeric films, which can be estimated from electrochemical and optical (by UV-vis spectroscopy) measurements and also from electronic structure calculations.

a 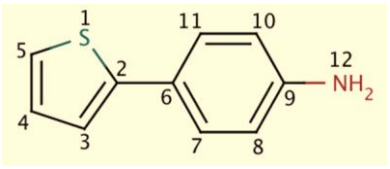

b 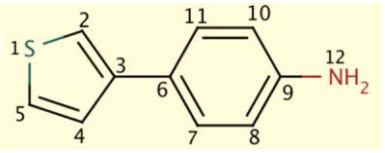

Figure 1. Chemical structure of the synthesized monomers, (a) 4-(2-thiophen)-aniline (4,2TA) and (b) 4-(3-thiophen)-aniline (4,3TA)

In this paper, the organic synthesis of the monomeric units 4-(2-thiophen)-aniline (4,2TA) and 4-(3-thiophen)-aniline (4,3TA) Figure 1, and their respective conducting polymers P4,2TA and P4,3TA, has been completed. In this work we report two new polymers containing aniline and thiophene moieties where aniline is electron-donating and thiophene can provide large light absorption and promote better π–π stacking/aggregation of polymeric chains leading to a small energy band gap[29].

2. EXPERIMENTAL DETAILS

All chemicals and solvents were purchased from *Aldrich*, and were utilized as received. Both monomeric units, 4,2TA and 4,3TA, Figure 1, were synthesized following the same procedure reported by *Suzuki-Miyaura* cross-coupling reaction[30,31] between 4-bromoaniline and 2-thyenil boronic acid or 3-thyenil boronic acid, respectively, in presence of 10 mol% Pd/C as catalyst and potassium carbonate to activate the catalyst. Subsequently, the monomers were purified and polymerized using H_5IO_6 and $HClO_4$ as oxidizing agent mixture[32]. All products were characterized using NMR and UV-vis spectroscopy. NMR spectra were recorded on a *Bruker* 400 MHz spectrophotometer using DMSO d_6 as solvent to determine the monomeric and polymeric structures and the polymerization positions.

UV-Vis measurements were carried out on a *CARY 5G* spectrophotometer. The polymer films were prepared by thermal evaporation (high vacuum sublimation) at $1x10^{-7}$ atm of pressure at the same time as the photovoltaic devices. The deposit rate of each polymer was 0.5 $Å \cdot s^{-1}$ and the film thickness was 140 Å. In order to investigate the optical behavior at the same conditions of the solar cell, the optical properties were determined in solid state (optical density O.D). P4,2TA and P4,3TA were deposited in undoped state to avoid quenching by recombination of charges in the photovoltaic devices. The optical energy gap (*Eg*) for each polymer (P4,2TA and P4,3TA) was obtained from the UV-vis spectra using an approximation of the *Tauc* equation[33-36]:

$$Eg = \frac{1242}{l_{onset}} \qquad (1)$$

where λ_{onset} is the wavelength threshold obtained from the UV-Vis spectra.

The electrochemical work was performed on a *Voltamaster* model CV 50W potenciostat/galvanostat, using a conventional three-compartment, three-electrode cell, and a polycrystalline platinum disk (0.07 cm^2 geometric area) as working electrode. The counter electrode was a coiled Pt wire of large area, separated from the electrolytic solution by a sintered glass. The reference electrode was a Ag/AgCl electrode that matches the potential of the saturated calomel electrode (SCE). Then all potentials quoted in the electrochemical section, are referred to the SCE. The electro-polymerization of each monomer (0.01 $mol \cdot L^{-1}$) was carried out in anhydrous acetonitrile using tetrabutylammonium hexafluorophosphate ($TBAPF_6$, 0.1 $mol \cdot L^{-1}$) as supporting electrolyte. All the system was kept under argon atmosphere and all measurements were performed at room temperature.

The photovoltaic devices were assembled in a multi heterojunction structure as follows: indium tin oxide (ITO)/ anode buffer layer / electron donor polymer (P4,2TA or P4,3TA) / fullerene (C_{60}) / bathocuproine (BCP) / Al[37]. All polymers were used in undoped state. The device was prepared by sublimation at $1x10^{-7}$ atm. The thin film deposition rates and thickness were estimated *in situ* through a quartz monitor. Electrical characterizations were performed with an automated I-V tester, in the dark and under sun global AM 1.5 simulated solar illuminations. Performances of photovoltaic cells were measured using a calibrated solar simulator (*Oriel* 300W) at 100 mW/cm^2 light intensity.

The morphology of the ITO surfaces was characterized by AFM with a Bio AFM JPK in the tappig mode. Measurements were achieved at room temperature, using the same pyramidal Si_3N_4 tip. The surface roughness R_{rms} (root mean square roughness) of each polymeric surface over the different buffer layer was evaluated with the AFM software.

The crystalline structure of the films was analyzed by X-ray diffraction (XRD) by a Siemens D 5000 diffractometer using Kα radiation from Cu (α=0.15406 nm)

3. RESULTS AND DISCUSSION

3.1. NMR characterization of monomers and polymers

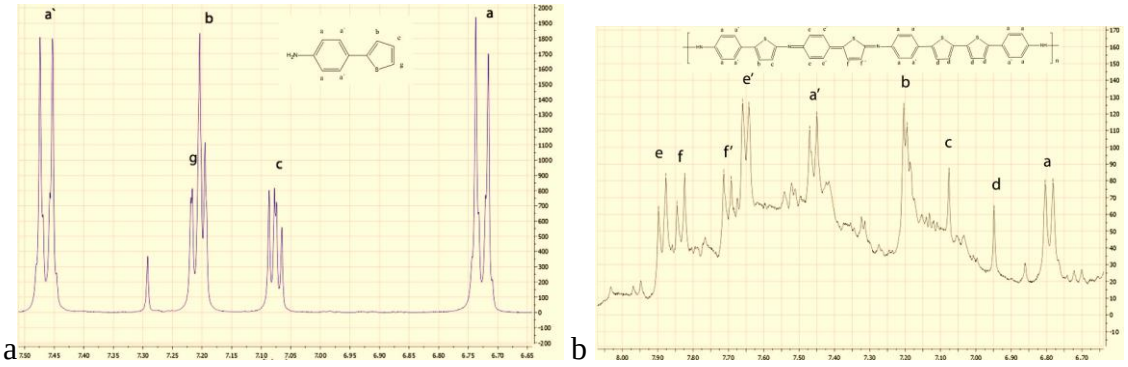

Figure 2. ^{1}H-NMR spectra in the aromatic range for (a) the monomer 4,2TA and (b) the polymer P4,2TA

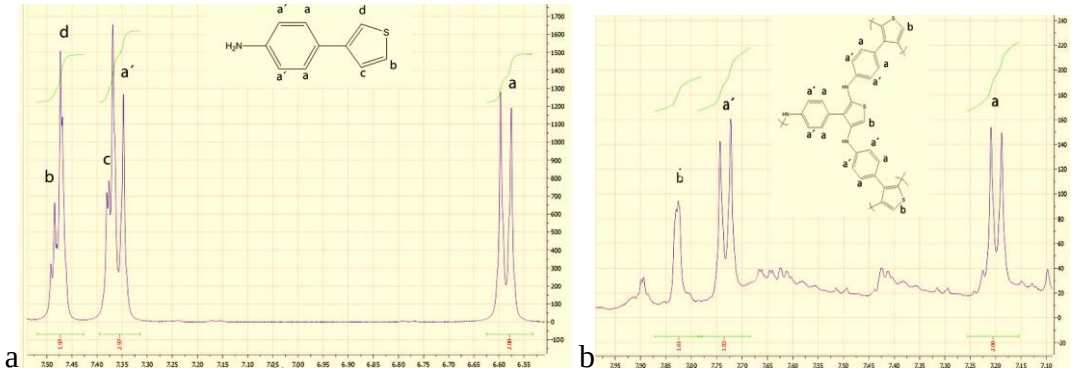

Figure 3. ^{1}H-NMR spectra in the aromatic range for (a) the monomer 4,3TA and (b) the polymer P4,3TA

The structure of the synthesized monomers and polymers was characterized through ^{1}H-NMR spectra, as Figure 2 and Figure 3 show. The ^{1}H-NMR spectra of 4,2TA and 4,3TA (in panels a) were confronted with ^{1}H-NMR spectra of their respective polymers, P4,2TA and P4,3TA (in panels b) in order to identify the positions, through signal disappearances, where 4,2TA and 4,3TA polymerized. The atomic numeration of both monomers is displayed in Figure 1.

The aromatic zone of the ^{1}H-NMR spectra of 4,2TA shows seven kinds of signals (Figure 2a): a´ and a, were assigned to protons belonging to the aniline aromatic ring. Signal c (C4) corresponds to a double doublet, which is coupled with signals b and g (C3 and C5, respectively of the thiophene ring). Notice that the ^{1}H-NMR spectra of P4,2TA in Figure 3b, shows similar signals as those presented in the 4,2TA spectra (a, a´, b and c). Additional signals can be identify due to the polymerization process and the presence of different oxidation states. The signals e, e´,f and f˝ were assigned to protons of the quinoidal rings of the polymeric chain[38]. The signal d was assigned to the C5-C5 linkage, based on a study previously reported by Le`re-Porte et al.[39]. Since the nitrogen-nitrogen linkage is not possible in this type of polymerization processes[1], only one C5-C5 bond per polymeric chain can exist. As can be seen, the signal g disappeared in the polymer spectra (proton of C5), which suggests that the polymerization reaction takes place between the nitrogen atom of aniline and the C5 of the thiophene ring, as well as between the C5 of two thiophene rings. Consequently, there are only two possible polymerization positions giving rise to a linear polymeric structure.

Figure 3a shows five kind of signals at the ^{1}H-NMR spectra of the aromatic region of the 4,3TA. a and a´ correspond to the protons of the aniline ring. The signal c is a doublet coupled with proton b (proton of the C4 and C5, respectively) and signal d is a singlet (proton of the C2). When 4,3TA was polymerized, the signals c and d of the monomer disappeared Figure 3b. This fact indicates that the polymerization occurs through C2 and C4 of the thiophene ring. No signals of C_{Th}-C_{Th} linkage (C2-C2, C4-C4 or C4-C2) or signals associated to quinoidal units were observed. Therefore, P4,3TA presents two possible sites of polymerization, which leads to the formation of a non-linear, and branched structure, without quinoidal units.

The ^{1}H-NMR spectra of 4,2TA, P4,2TA, 4,3TA, and P4,3TA are summarized below:

4,2TA: ^{1}H-NMR (400 MHz, DMSO d_6) δ 3.76 ppm (s. 2H, N-H); 6.72 ppm (d. 2H, Ha); 7.07 ppm (dd. 1H; Hc); 7.20 ppm (d. 1H, Hb); 7.22 ppm (d. 1H, Hg); 7.47 ppm (d. 2H, Ha´).

P4,2TA: ^{1}H-NMR (400 MHz, DMSO d_6) δ 3.25 ppm (s. N-H); 6.78 ppm (d. 2H, Ha); 6.95 ppm (s. 2H, Hd); 7.08 ppm (s. 1H, Hc); 7.20 ppm (m. Hb); 7.45 ppm (d, 2H, Ha´); 7.64 ppm (d, 2H, Ha´); 7.64 ppm (d. 2H, H-e´); 7.70 (d. 2H, Hf´); 7.82 ppm (d, 2Hf); 7.88 ppm (d. 2H, He).

4,3TA: ^{1}H-NMR (400 MHz, DMSO d_6) δ 5.13 ppm (s. 2H, N-H); 6.57 ppm (d. 2H, Ha); 7.35 ppm (d. 2H, Ha´); 7.38 ppm (d. 1H, Hc); 7.47 ppm (d. 1H, Hd); 7.49 ppm (d. 1H, Hb).

P4,3TA: ^{1}H-NMR (400 MHz, DMSO d_6) δ 3.91 ppm (s. N-H); 7.19 ppm (d. 2H, Ha); 7.72 ppm (d. 2H, H-a´); 7.83 ppm (s. 1H, Hb).

3.2. Optical Properties

Figure 4 depicts the UV-Vis absorption spectra of each polymer: P4,2TA and P4,3TA. P4,2TA presents absorption bands at higher wavelength than P4,3TA, therefore, 4,2TA polymer is more energetically stable than the P4,3TA. This red-shifting is observed due to the presence of different oxidation states into the polymeric chain, like the quinoidal units, and the semi-planar and non-branched structure of P4,2TA, which leads to a more conjugated polymer[40-42].

Figure 4. UV-Vis absorption spectra of P4,2TA and P4,3TA

On the other hand, P4,2TA shows three distinctive absorption maxima corresponding to π-π* benzenoid electronic transitions close to 350 nm, π-π* thiophene ring electronic transition at 450 nm and the characteristic π-π* quinoidal electronic transitions are observed at about 700 nm, according with the ^{1}H-NMR spectra. Between 650 nm and 800 nm, n-π* transitions were registered and assigned to the transition of the electrons at the nonbonding orbital of the imino nitrogen atom formed by the quinoidal type structure[33]. These electronic transitions were not considered in the *Eg* calculation. In this wavelength range n-π* transitions also exist owing to electrons in nonbonding orbitals of the imino nitrogen formed by the quinoid rings[33].

Unlike P4,2TA, P4,3TA shows only two absorption maxima corresponding to π-π* benzenoid electronic transitions at around 300 nm and π-π* thiophene ring electronic transition at 400 nm. Notice that no quinoidal transitions in the range of 650 nm - 800 nm were observed.

Table 1. Experimental (UV-vis) values of HOMO, LUMO and the optical bang gap (*Eg*) of P4,2TA and P4,3TA. All values in eV.

	-HOMO (eV)	-LUMO (eV)	Eg (eV)
P4,2TA	4.9	3.1	1.8
P4,3TA	5.1	3.0	2.1

Figure 4**Error! Reference source not found.** and Eq. 1 were employed to calculate the optical band gap of both polymers. As Table 1 shows, P4,2TA presents the lowest value according to a greater delocalization of electronic charge comparing to P4,3TA. This fact demonstrates that blocking the C2 of the thiophene ring, ensures a polymerization process through the C5, generating quinoidal structures along the polymeric chain and higher π-conjugation.

3.3. Electrochemical Properties

The electrochemical polymerization and deposition of P4,2TA and P4,3TA, was carried out from solutions containing 0.01 mol·L^{-1} monomer and $TBAPF_6$ 0.1 mol·L^{-1} supporting electrolyte.

Polymerization was achieved by cyclic voltammetry (potentials between 0.0 and 1.4 V, 50 $mV \cdot s^{-1}$ scan rate). Polymeric responses were assessed applying a perturbation to the modified electrode in a monomer-free solution of anhydrous acetonitrile finding in both cases only a p-type doping. No chemical degradation of this state was observed after 10 cycles. Figure 5 displays the fourth voltammetric cycle.

To estimate the HOMO energy, the slope change of the anodic current was determined, as figure 5 shows. This value corresponds to the onset oxidation potential (Eox)on, and correlates linearly with the HOMO energy (E_{HOMO}), with a correction factor of 4.4 eV[43-50].

$$E_{HOMO} = -((Eox)on + 4.4)eV \quad (2)$$

HOMO values are quoted in Table 1. As expected, the P4,2TA HOMO is higher than P4,3TA HOMO by 0.2 eV, because of its superior stability and electronic conjugation. These results showed that the HOMO levels of the polymers significantly depend on the molecular geometry and chemical structure of polymeric chains.

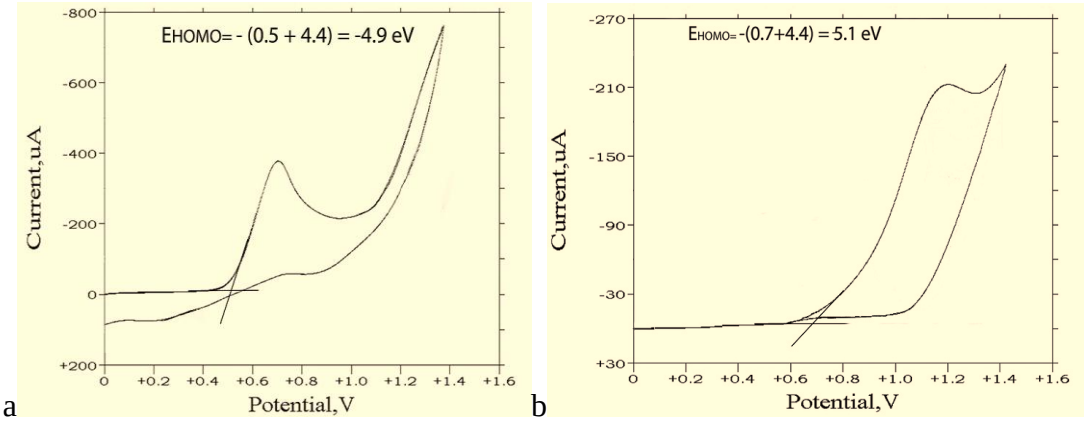

a b

Figure 5. Voltammetric profile of (a) P4,2TA (b) P4,3TA. Interface Pt | TBAPF6 (0.1 $mol \cdot L^{-1}$) in CH_3CN. Scan rate 50 $mV \cdot s^{-1}$, cycle 4

It was not possible to determine through electrochemical measurements the onset reduction potential (Ered)on. When electrons were injected, a chemical degradation of the film occurred, and the n-doped state was destroyed. Thus, to determine the LUMO energy, Eq. 3 was used[51]. Values are also summarized in Table 1.

$$E_{LUMO} = E_{HOMO} - E_g \quad (3)$$

3.4. Photovoltaic performance of P4,2TA and P4,3TA

Figure 6 depicts the photovoltaic properties of each polymer, placed by high vacuum deposition on a ITO/CuI buffer layer. The photovoltaic yield of the P4,2TA-cell is around 100 times

higher than the device fabricated with P4,3TA Table 2. As NMR, UV-vis spectroscopy and electrochemical analysis showed, P4,2TA is a linear polymer.

Table 2. Prameters of the solar cell on CuI buffer layer

Polymer	Voc (V)	Jsc (mA/cm^2)	FF (%)	η (%)
P4,2TA	0,20	4,13	32,9	0,23
P4,3TA	0,40	0,79	23,4	5,4x10^{-2}

This semi-planar geometry provides better contact with the buffer layer and facilitates the charge inter-chain transfer due to lower electrical resistance, giving rise to a bigger short circuit current (J_{sc}), unlike P4,3TA. Due to the greater energetic difference between the HOMO level of the electron donor and the LUMO energy of the electron acceptor (fullerene C_{60}, 3.78 eV[52]), the open circuit potential (Voc) of P4,3TA was higher than the Voc of P4,2TA and the photovoltaic performances are in accordance with the proposed molecular geometry. However, to better understand the origin of the photovoltaic performance difference in the photovoltaic cells AFM images and XRD were collected. As shown in Figure 7 the roughness variation of the polymer film influences its optical properties, which will influence the final electrical characteristics of the solar cell, in this sense the reduction of the Jsc respect the roughness could be related to an. incomplete carrier collection at the p-n junction when the polymer surface is smoother (P4,3TA surface) producing enhancement of reflectivity of polymeric film[53].

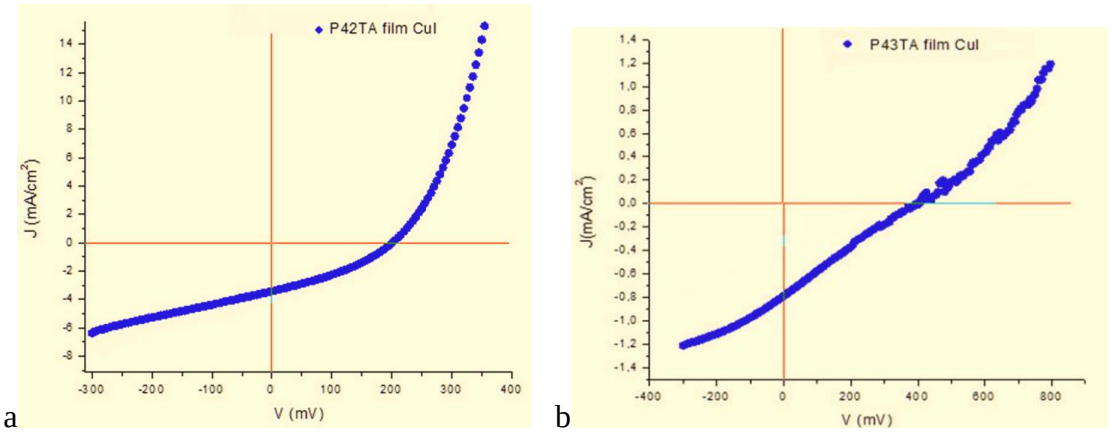

a b

Figure 6. Graphic current density v/s voltage of solar cell on CuI buffer layer a) P4,2TA b) P4,3TA

P4,2TA presents a rougher surface and peaks and valleys homogeneously dispersed, allowing better contact and charge transference between P4,2TA and C60. Unlike the surface of P4,3TA presents large grains separated by smooth areas. This type of topography can be attributed to the branched molecular geometry of P4,3TA, which would facilitate the formation of granular

agglomerates distributed in non-homogeneous form. Moreover, the molecular geometry of P4,2TA facilitates the growth of small peaks, due to the existence of higher order in the polymer chains, this is supported by the results of XRD.

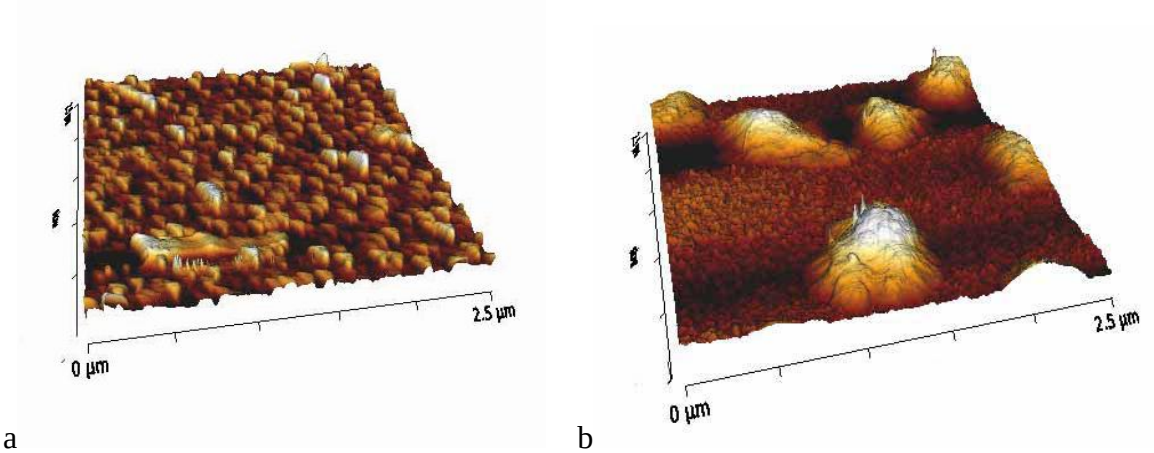

a b

Figure 7 AFM topography images (a) P4,2TA (b) P4,3TA

Figure 8 shows the XRD patterns of P4,2TA and P4,3TA. It can be seen that the polymer P4,2TA with linear molecular geometry gives XRD peak in the low-angle region 12° (d_1=7.16A°), and one XRD peak at about 22° (d_2=4.04A°). π-Conjugated polymers, including thiophene-based □-conjugated polymers, often show similar XRD patterns. The peak in the low-angle region is assigned to the distance between π-conjugated polymer main chains. The d_2 peak of about 4.04A° is reasonable for a stacking distance of thiophene-based π- conjugated polymers[54-60]. The XRD pattern between 17° and 40° showed peaks at 25° and 30° corresponds to XRD signals of ITO conducting glass, suggesting that there are an amorphous packing of the polymer molecules. Figure 9 shows a possible alignment of layers of the deposit of P4,2TA

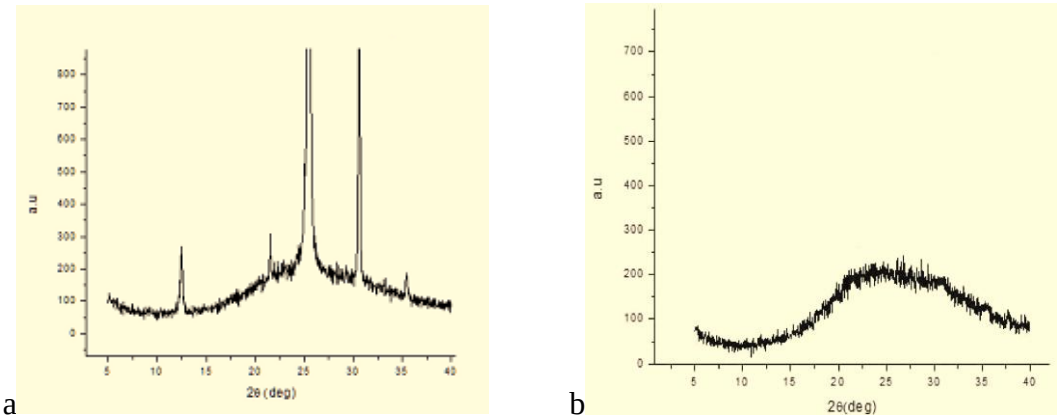

a b

Figure 8. X- ray diffraction spectrum (a) P4,2TA (b) P4,3TA

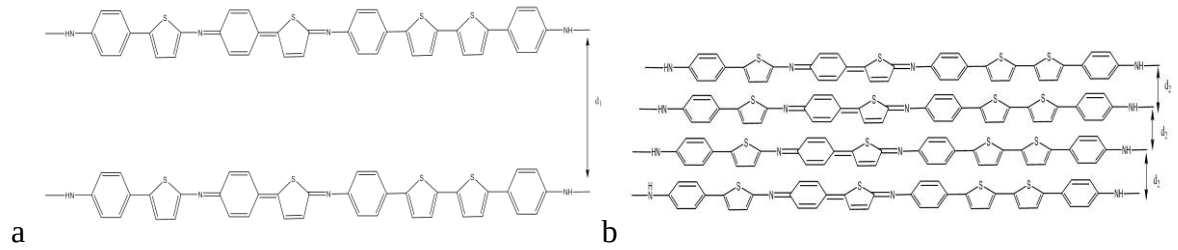

Figure 9. (a)Schematic diagram of packing mode with interchain distance d1. Sheets formed are considered to form a stacked assembly. (b) Layered structure with face-to-face stacking.

There are no peaks observed in the diffraction pattern of P4,3TA leaving a broad structured peak centered at about 25°, due to the amorphous component in the sample. This fact produces a surface with scattered agglomerates, not homogeneous and areas of low roughness.

The XRD results of P4,2TA confirm the existence of a deposit with crystalline regions, leading to higher carrier mobility and the formation of a homogeneous rough surface.

It is important to point out that the weight average molecular weight (M_w) and number average molecular weight (M_n) were not determined since there is uncertainty about the size of the polymer chains deposited in the solar cell. It is possible that during the sublimation process, the polymer is divided in shorter oligomeric chains. In order to check the sublimation effects, two P4,2TA polymer surfaces were produced via spin coating and high vacuum sublimation. UV-vis spectra of both P4,2TA were taken displayed in Figure 10. The polymer deposited by sublimation exhibited a blue shift, directly related to the loss of conjugation due to the decrease of the chain length. In spite of the above, optical properties of the polymer were not affected.

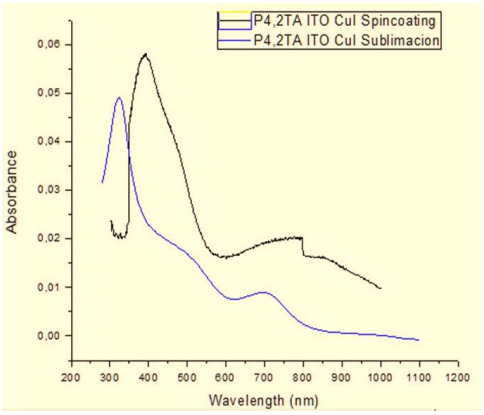

Figure 10. Optical density of P4,2TA spincoating (Black), sublimation (red)

4. CONCLUSIONS

Spectroscopic characterization indicates the chemical polymerization of 4-(2-thiophen) aniline monomer proceeds through the amino nitrogen atom and carbon 5 of the thiophene ring, giving a linear

polymer structure, while for 4-(3-thiophen) aniline polymerization occurs through the nitrogen atom and carbons 2 and 4 of the heterocycle, yielding a branched product. The difference between both structures is reflected in their optical and electronic properties, being P4,2TA the one showing the highest efficiency when the photovoltaic device is made . Their three dimensional conformation would enable the contact with the buffer layer being more suitable than with P4, 3TA.

P4,2TA shows a surface rougher than P4,3TA surface and deposits more crystalline, which leads to better performance photovoltaic.

ACKNOWLEDGMENTS

The authors thank FONDECYT financial support through project 1095156. I.J. and P.Z. acknowledge the doctoral scholarship 21090478, doctoral scholarship support 24110046, granted to conduct this research and ECOS CONICYT project No.C09E02

References

1. S. Bhadra; N. Singha; D. Khastgir, *Eur. Polym. J*, 44 (2008) 1763.
2. Z. Liu; W. Guo; D. Fu.; W. Chen, *Synth. Met,* 156 (2006) 414.
3. J. Gao; J. M. Sansinena; H. L. Wang, *Synth. Met,* 135 (2003) 809.
4. A. Bishop; P. Gouma, *Rev. Adv. Mater. Sci,* 10 (2005) 209.
5. Y. Kaminorz; E. Smela; T. Johansson; L. Brehmer; M. R. Andersson; O. Inganäs, *Synth. Met,* 113 (2000) 103.
6. P. Bäuerle; U. Segelbacher; A. Maier; M. Mehring, *J. Am. Chem. Soc,* 115 (1993) 10217.
7. G. Barbarella; L. Favaretto; G. Sotgiu; P. Zambianchi; A. Bongini; C. Arbizzani; M. Mastragostino; M. Anni; G. Gigli; R. Cingolano, *J. Am. Chem. Soc,* 122 (2000) 11971.
8. F. Geiger; M. Stoldt; H. Schweizer; P. Bäuerle; E. Umbach, *Adv. Mater,* 5 *(*1993) 922.
9. P. Ho; J. S. Kim; J. H. Burroughes; H. Becker; S. F. Li; T. M. Brown; F. Cacialli; R. H. Friend, *Nature,* 404 (2000) 481.
10. O. Inganäs; M. Berggren; M. Andersson; G. Gustafsson; T. Hjertberg; O. Wennerström; P. Dyreklev; M. Granström, *Synth. Met,* 71 (1995) 2121.
11. Y. Kaminorz; E. Smela; O. Inganäs; L. Brehmer, *Adv. Mater, 10 (*1998) 76.
12. D. J. Pinner; R. H. Friend; N. Tessler. *Appl. Phys. Lett,* 76 (2000) 1137.
13. L. Ding; M. Jonforsen; L. S. Roman; M. R. Andersson; O. Inganäs, *Synth. Met,* 110 (2000) 113.
14. M. Granström; K. Petrisch; A. C. Arias; A. Lux; M. R. Andersson; R. H. Friend, *Nature,* 395 (1998) 257.
15. H. Hoppe; N. S. Sariciftci; *J. Mater. Res,* 19 (2004) 1924.
16. T. Otsubo; Y. Aso; K. Takimiya, *Bull. Chem. Soc. Jpn.,* 74 (2001) 1789.
17. A. Salomon; D. Cahen; S. Lindsay; J. Tomfohr; V. B. Engelkes; C. D. Frisbie, *Adv. Mater,* 15 (2003) 1881.
18. A. Dodabalapur; H. E. Katz; L. Torsi; R. C. Haddon, *Science,* 269 (1995) 1560.
19. F. Garnier; R. Hajlaoui; A. Yassar; P. Srivastava, *Science,* 265 (1994) 1684.
20. F. Garnier; *Chem. Phys,* 227 (1998) 253.
21. G. Horowitz; X. Peng; D. Fichou; F. Garnier, *J. Appl. Phys,* 67 (1990) 528.
22. R. E. Matin; F. Diederich, *Angew. Chem. Int. E,* 50 (1999) 1350.
23. N, Robertson; C. A. McGowan, *Chem. Soc. Rev,* 32 (2003) 96.
24. F, Würthner, *Angew. Chem. Int. Ed. Engl,* 40 (2001) 1037.
25. A. K. Bakhshi; K. Sangeeta, *Appl. Biochem. Biotechnol,* 96 (2001) 125.
26. Z. Zhu; D. Waller; R. J. Gaudiana, *Macromol. Sci., Pure App. Chem,* 44 (2007) 1249.

27. Y. Ooyama; Y. Harima, *Eur. J. Org. Che, 18 (*2009) 2903.
28. N, Armstrong, C. Carter, C. Donley, *Thin Solid Films, 445 (*2003) 342.
29. P. Xia, X. Feng, J. Lu, *Adv. Mater*, 1 (2008) 9999.
30. F. Felpin, *J. Org. Chem*,70 (2005) 857.
31. J. Ryu; C. Jang, *J. Org. Chem*, 70 (2005) 8956.
32. M. Can; S. Uzuna; N. Pekmez, *Synth. Met*, 159 (2009) 1486.
33. V. Bavastrello; S. Carrara, *Langmuir*, 20 (2004) 969.
34. K. Colladeta; M. Nicolasa, *Thin Solid Films*, 7 (2004) 451.
35. W. Feng; Z. Qi; Y. Sun, *J. Appl. Pol. Sci*, 104 (2007) 1169.
36. J. Kong; E. Lim; K. Lee, *Sol. Energ. Mater. Sol. C,* 94 (2010) 2057.
37. Y. Berredjem; N. Karst; L. Cattin, *Dyes Pigments*, 7 (2006) 351.
38. I. Mav; M. Žigon, *Polym. Bull*, 45 (2000) 61.
39. J. J. Lère-Porte; J. J. E. Moreau; C. Torreilles, *Eur. J. Org. Chem*, 5 (2001) 1249.
40. L. Dai, *Macromol. Chem. Phys*, 2 (1999) 273.
41. C. O. Sánchez; C. J. Bustos, *Polym. Bull*, 54 (2005) 263.
42. S. Günes; H. Neugebauer, *Chem. Rev*, 107 (2007) 1324.
43. A. Charasab; J. Morgado, *Polymer*, 44 (2003) 1843.
44. J. Pei; W. Yu, *Macromolecules*, 34 (2001) 7241.
45. P. K. Hegde; A. D. V. Adhikari, *Synth. Met*, 159 (2009) 1099.
46. Q. Zhang; Y. Li; M. Yang, *J. Mater. Sci*, 39 *(*2004) 6089.
47. A. Charas; J. Morgado; J. Martinho; L. Alcácer; S. Lim; R. Friend; F. Cacialli, *Polymer*, 44 (2003) 1843.
48. S. Admassie; O. Inganas; W. Mammo; E. Perzon; M. Andersson, *Synth. Met*, 156 (2006) 614.
49. P. K. Hegde; A. V. Adhikari; M. G. Manjunatha; C. S. Suchand; R. Philip, *Synth. Met*, 159 (2009) 1099.
50. E. Zhou; M. Nakamura; T. Nishizawa; Y. Zhang; Q. Wei; K. Tajima; C. Yang; K. Hashimato. *Macromolecules*, 41 (2008) 8302.
51. M. JuCho, J. Seo, *Sol. Energ. Mater, 98 (*2012) 71.
52. D. Mi; H. Kim; J. Kim, *Synth. Met*, 162 (2012) 483.
53. Z. Jehl, M. Bouttemy, D. Lincot, *J. Appl. Phys*, 111 (2012) 114509; doi: 10.1063/1.4721648
54. R. McCullough; S. Tristam-Nagle; S. Williams, *J. Am. Chem. Soc*, 115 (1993) 4910.
55. H. Sirringhaus; P. Brown; R. Friend; M. Nielsen, *Nature*, 401 (1999) 685.
56. I. McCulloch; M. Heeney; C. Bailey; K. Genevicius, *Nat. Mater*, 5 (2006) 328.
57. J. Li; F. Qin; C. Li; Q. Bao; M. Chan-Park, *Chem. Mater*, 20 (2008) 2057.
58. T. Yamamoto; H. Ootsuka; T. Iijima, *Macromol. Rapid Commun*, 28 (2007) 1786.
59. T. Yamamoto; Q. Fang ; T. Morikita, *Macromolecules*, 36 (2003) 4262.
60. S. Morita; S. Kiyomatsu; X. Yin; H. Xiao; A. Zakhidov, *J. Appl. Phys*, 74 (1993) 2860.